Semaphorin 3E-Plexin-D1 signaling controls pathway-specific synapse formation in the striatum

Jun B. Ding[1,2,3], Won-Jong Oh[1,3], Bernardo L. Sabatini[1, 2*], Chenghua Gu[1*]

[1]Department of Neurobiology, [2]Howard Hughes Medical Institute, Harvard Medical School, 220 Longwood Ave, Boston, MA 02115, [3]These authors contributed equally to this work.

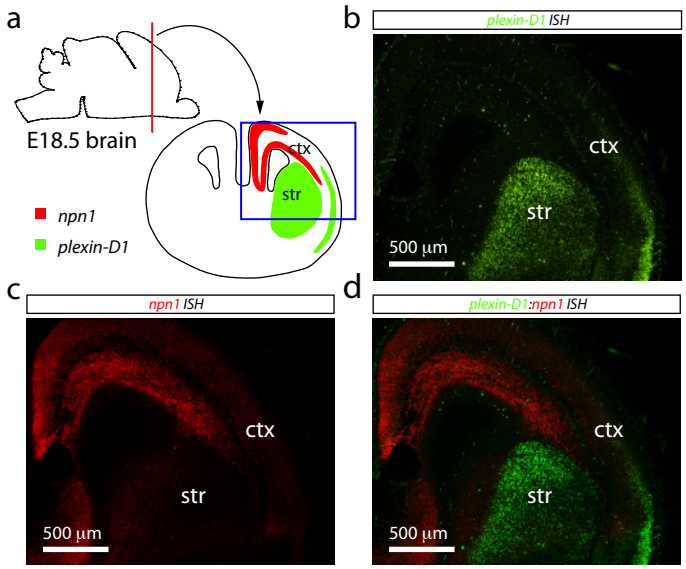

Supplementary Figure 1. *npn1* is not expressed in the striatum.
(**a**) Schematic of a coronal brain slice and summary of the expression of *neuropilin 1* (red, *npn1*) and *plexin-D1* (green) in E18.5 mouse brain. (**b-c**) Double fluorescence in situ hybridization showing the expression of *plexin-D1* (**b**) and *npn1* (**c**). *plexin-D1* is highly expressed in the striatum, whereas *npn1* expression is absent. (**d**) Merged image shows complementary expression patterns of *plexin-D1* and *npn1* in the cortex (Ctx) and striatum (Str).

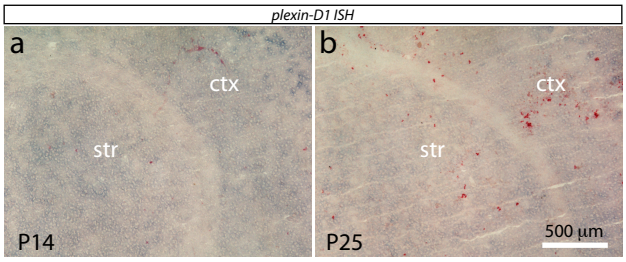

Supplementary Figure 2. Expression of *plexin-D1* in P14 and P25 mice.
In situ hybridization showing *plexin-D1* expression at P14 (**a**) and P25 (**b**) in the striatum. The *plexin-D1* expression level has significantly declined in P14 and P25 mouse striata as compared to P0-P8 mouse striata (**Fig. 1**).

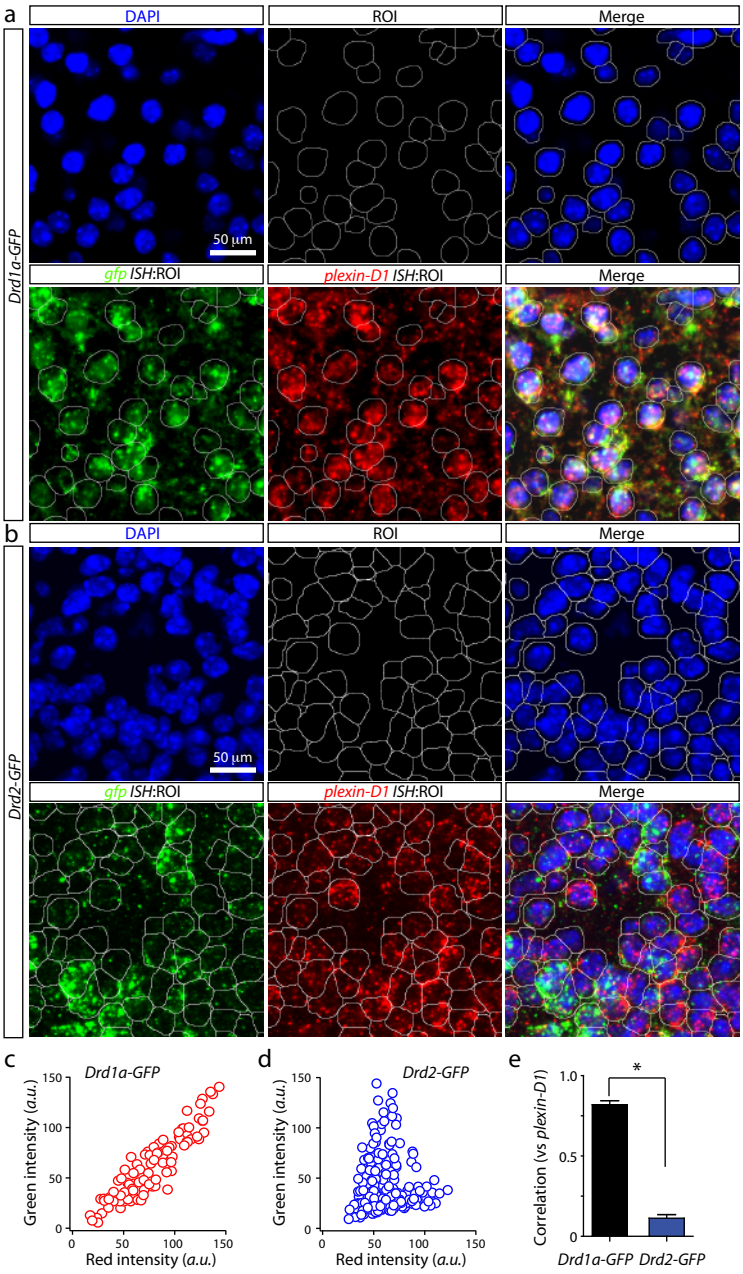

Supplementary Figure 3. Quantification of *plexin-D1* expression in direct and indirect pathway striatal MSNs.

(**a**) Double in situ hybridization of *gfp* (green) and *plexin-D1* (red) demonstrating co-localization of *gfp* and *plexin-D1* expression in *Drd1a*-GFP mice. To quantitatively analyze co-expression, DAPI fluorescence (blue) was used to identify individual neurons and define regions of interest (ROI) for quantification. Average *gfp* (green) and *plexin-D1* (red) ISH fluorescence in the same ROIs was compared on a cell-by-cell basis. (**b**) Similar analysis was performed in *Drd2*-GFP mice using identical conditions. (**c**) *gfp* fluorescence intensity from individual striatal neurons from *Drd1a*-GFP mice was plotted against their *plexin-D1* fluorescence intensity. Each circle represents an individual neuron. (**d**) *gfp* fluorescence intensity from individual striatal neurons from *Drd2*-GFP was plotted against their *plexin-D1* fluorescence intensity. (**e**) Quantification of the correlation coefficients of *gfp* and *plexin-D1* expression in *Drd1a*- and *Drd2*-GFP mice ($P<0.05$; Mann-Whitney).

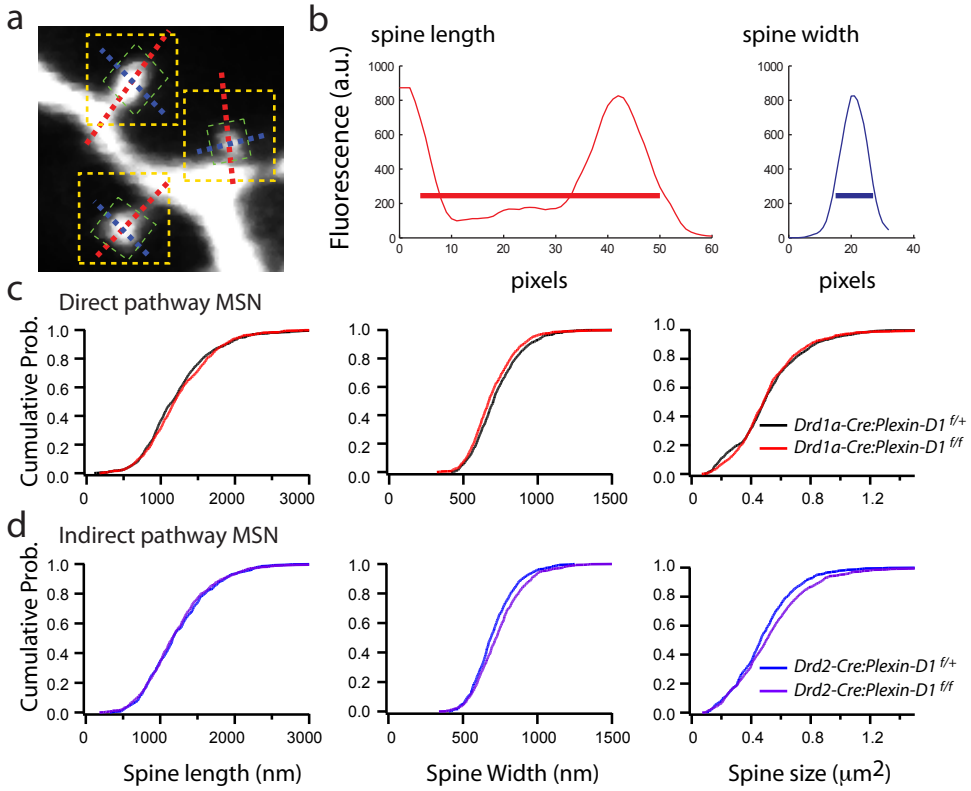

Supplementary Figure 4. Spine morphology is not altered in *plexin-D1* conditional knockout mice.

(**a**) Image of dendritic spines indicating the method of morphometric analysis. The major (red line) and intersecting minor (blue line) axes were marked along the length and the width of each spine. The green box indicates the area containing the spine head. The pixels within this box whose fluorescence intensities are at least 50% of the maximal value are used to define the area of the spine head. (**b**) The distances to 30% of maximal fluorescence along the major and minor axis were used to define, respectively, the spine length (thick red line) and head width (thick blue line). (**c**) Comparison of spine length (*left*), head width (*middle*), and head area (*right*) of direct pathway MSNs in *Drd1a*-Cre;*Drd2*-GFP;*plexin-D1*$^{f/f}$ and littermate control mice. (**d**) Comparison of spine length (*left*), head width (*middle*), and head area (*right*) of indirect pathway MSNs in *Drd1a*-Cre;*Drd2*-GFP;*plexin-D1*$^{f/f}$ and littermate control mice. There are no significant differences in spine morphology between control and *plexin-D1* conditional knockout MSNs (P>0.05; Mann-Whitney).

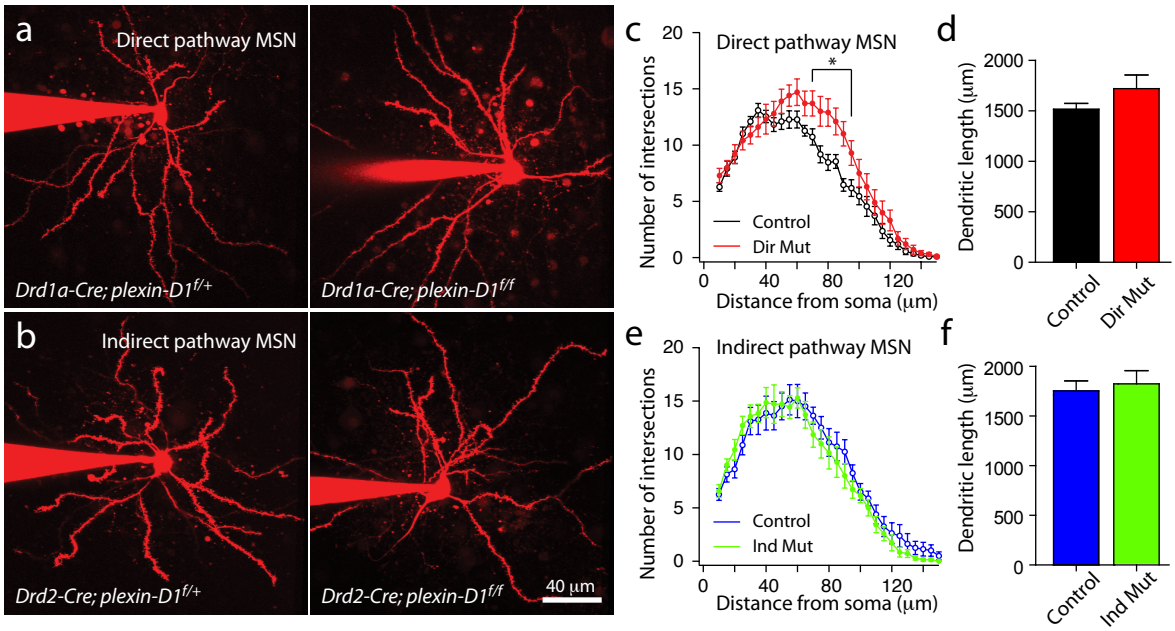

Supplementary Fig. 5. Alterations in dendritic length and branching in direct pathway and indirect pathway plexin-D1 mutant mice.
(**a-b**) 2PLSM images of dye-filled direct (**a**) and indirect (**b**) pathway MSNs from het control (*top*) and mutant (*bottom*) mice. (**c**) Scholl's concentric analysis shows that the number of dendritic intersections with somatically centered circles of increasing radius (5 μm increments) was slightly increased in direct pathway MSNs from direct pathway plexin-D1 mutant mice. * indicates $P<0.05$; n=10 cells in control and 11 in direct pathway mutant mice; Mann-Whitney. (**d**) There is no significant increase in total dendritic length in direct pathway MSNs from direct pathway mutant mice. (**e-f**) Similar analysis in indirect pathway MSNs shows no significant change in either dendritic branching or total dendritic length in indirect pathway MSNs from indirect pathway *plexin-D1* mutant mice, $P>0.05$; n=8 cells in control and 7 in indirect pathway mutant mice; Mann-Whitney.

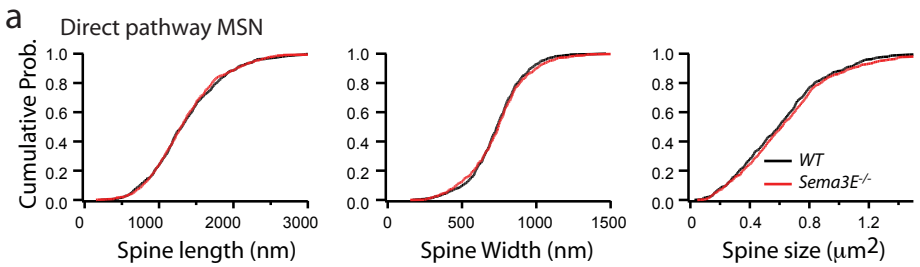

Supplementary Figure 6. Loss of *sema3E* does not alter spine morphology.
(**a**) Comparison of spine length (*left*), head width (*middle*), and head area (*right*) of direct pathway MSNs in wild-type (WT) and *sema3E*$^{-/-}$ mice. There are no significant differences in spine morphology between control and *sema3E*$^{-/-}$ MSNs (P>0.05; Mann-Whitney).

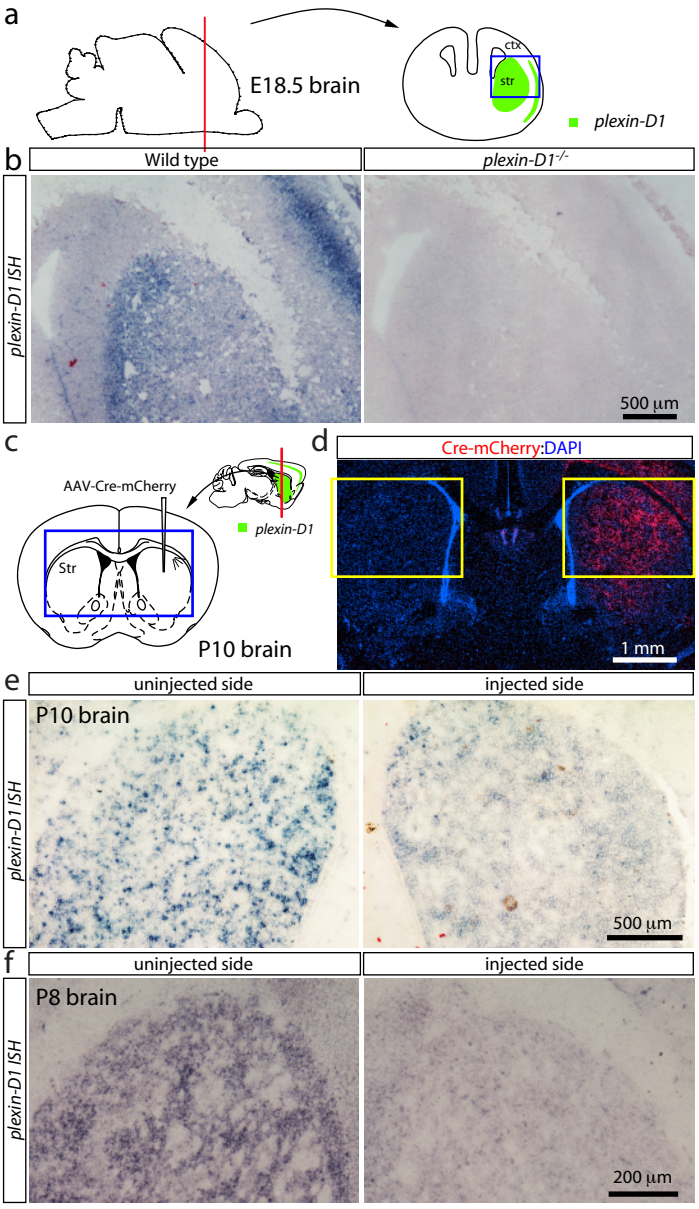

Supplementary Figure 7. Deletion of *plexin-D1* in striatal neurons using injection of AAV-Cre-mCherry.
(**a**) Schematic of a coronal brain slice. (**b**) In situ hybridization showing *plexin-D1* expression in E18.5 wild-type and *plexin-D1* null (*plexin-D1*$^{-/-}$) mice. (**c**) Schematic of brain slice depicting the virus injection site in the striatum. (**d**) Section from a *plexin-D1*$^{f/f}$ mouse stereotaxically injected with AAV-Cre-mCherry on P4 demonstrating robust expression of Cre-mCherry in the striatum 6 days after virus delivery (P10). Blue: DAPI, Red: mCherry. (**e**) In situ hybridization analysis of *plexin-D1* expression at P10 in the striatum from uninjected (**c**) and injected sides (**d**) showing clear down-regulation of *plexin-D1* 6 days after virus injection. (**f**) In situ hybridization analysis of *plexin-D1* expression at P8 in the striatum from uninjected (*left*) and injected sides (*right*) showing clear down-regulation of *plexin-D1* 4 days after virus injection.

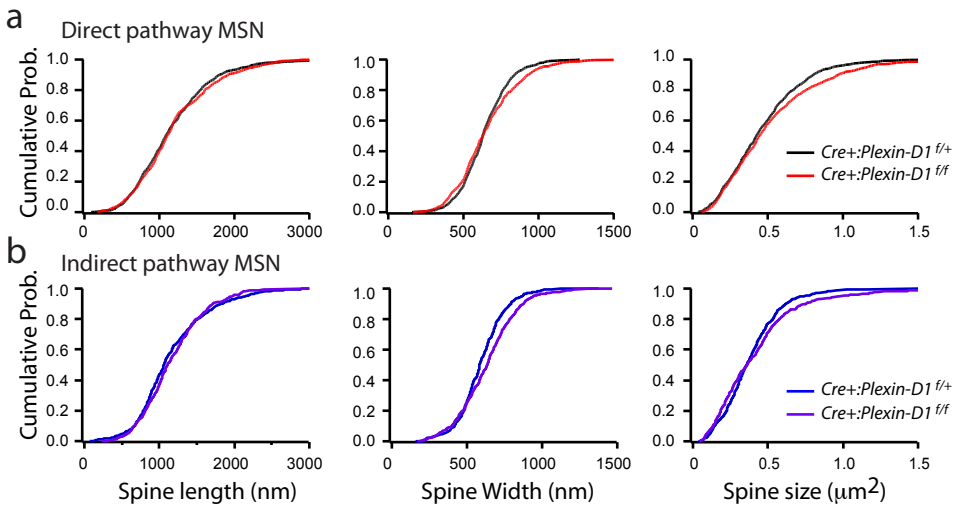

Supplementary Figure 8. Loss of *plexin-D1* does not alter spine morphology. (**a-b**) Comparison of spine length (*left*), head width (*middle*), and head area (*right*) in *plexin-D1* conditional KO direct pathway MSN (**a**) and indirect pathway MSNs (**b**). There are no significant differences in spine morphology between control and AAV-Cre-mCherry infected MSNs ($P>0.05$; Mann-Whitney).

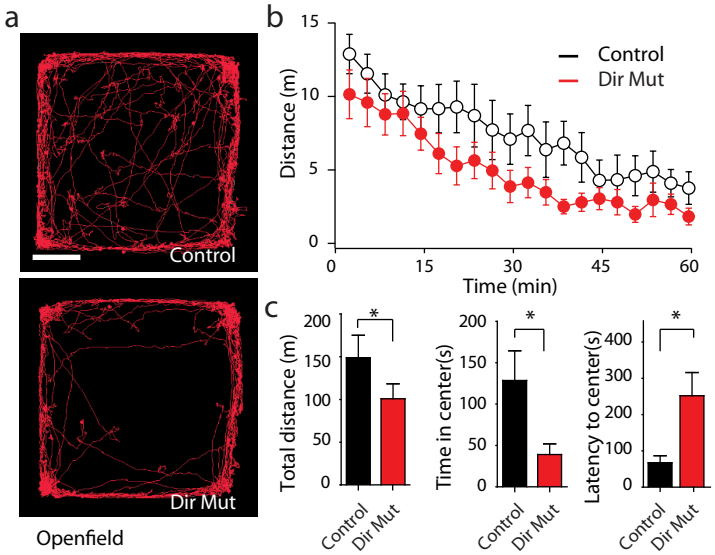

Supplementary Figure 9. Basal locomotor activity is altered in direct pathway *plexin-D1* mutant mice.

(**a**) Direct pathway *plexin-D1* conditional null mice and their same-sex littermate controls (7-10 weeks old) were individually placed into an open field chamber (44 cm × 44 cm) for an hour. Locomotion was measured by recording the distance traveled over a 60-min period. Examples of position tracking over the first 10 minutes are shown in red for control (*top*) and *plexin-D1* direct pathway mutant mice (*bottom*). (**b**) Distance traveled (in meters) was plotted against time in 3-min bins over a 60 min period for mice of the indicated genotypes (red filled circles, direct pathway *plexin-D1* mutant; open circle, littermate controls). (**c**) Bar graphs summary showing the average total distance traveled over the 60-min period (in meters, *left*); time spent in the center quadrant (*middle*) and latency for mice to enter the center quadrant (*right*). * indicates statistical significance, $P<0.05$; n= 10 (6 males and 4 females control/mutant pairs), Wilcoxon. In addition to decreased total travel distance, the direct pathway *plexin-D1* null mice spent significantly less time in the center quadrant of the open field and it took significant longer time for the mutant mice to first enter the center quadrant of the open field.